Energy transfer process in unsymmetrical crown-containing bisstyryl dye incorporated in the cavities of CB[7] and 2-hydroxypropyl-β-CD

Anna Y. Ruleva, Vladimir B. Tsvetkov, Yuri V. Fedorov, Ekaterina Y. Chernikova, Nikolay E. Shepel, Ivan A. Godovikov, Olga A. Fedorova

Content

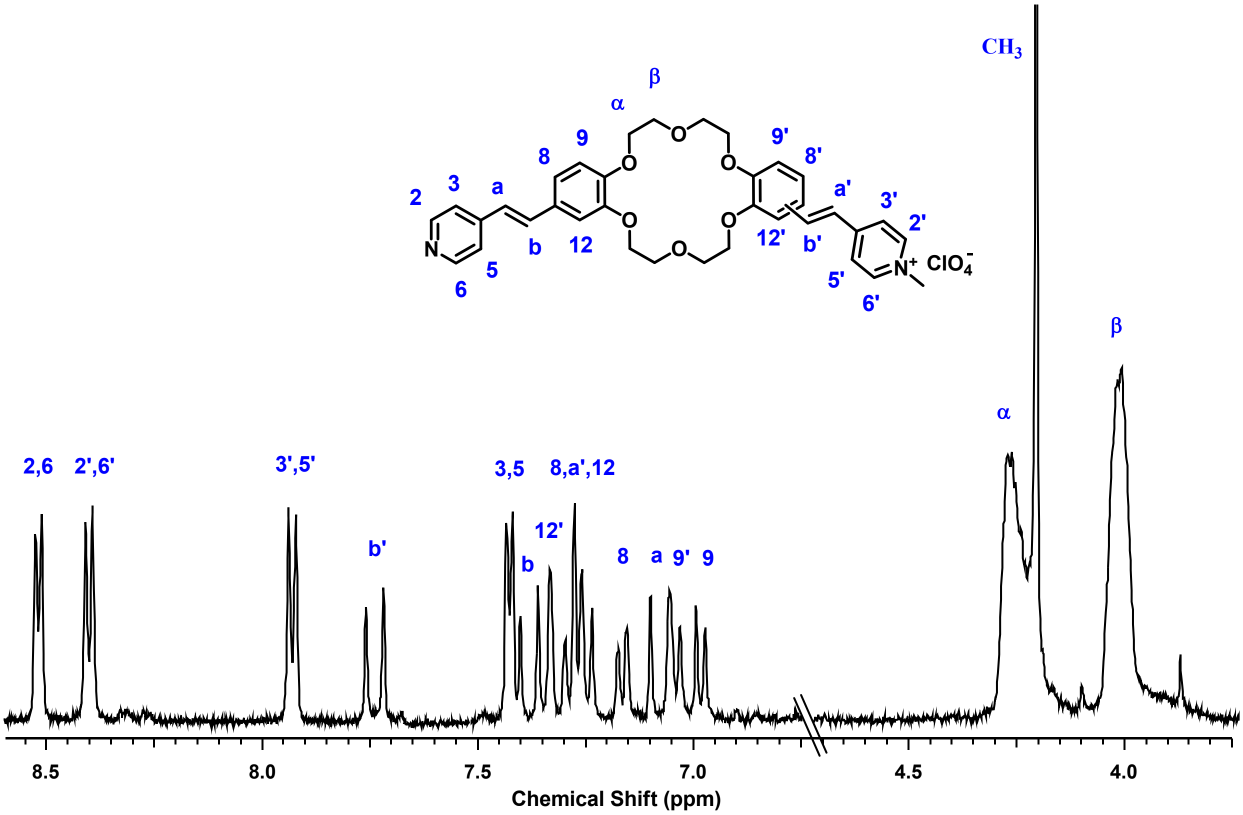

Fig. S1. – [1]H NMR spectra of bisstyryl dye **1** in CD_3CN.

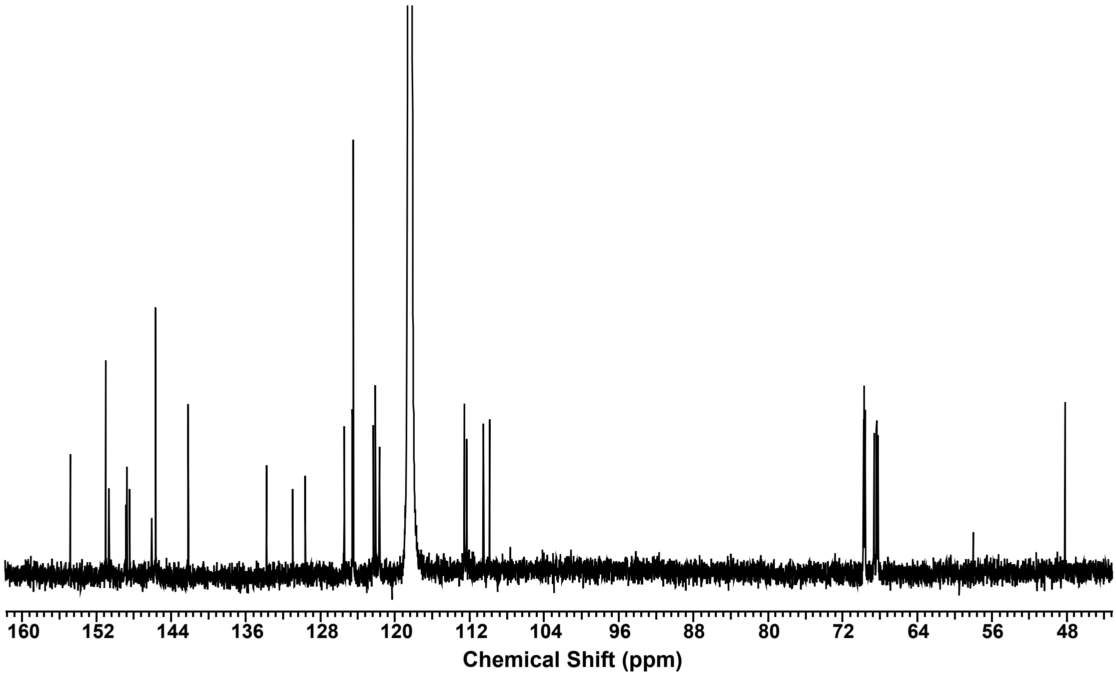

Fig. S2. – [13]C NMR spectra of bisstyryl dye **1** in CD_3CN.

Figure S3. Fragments of the COSY spectrum of free **1** (400 MHz, 298 K, D_2O-CD_3CN (3:1), $C_{\mathbf{1}}$ = $2\cdot10^{-3}$M)

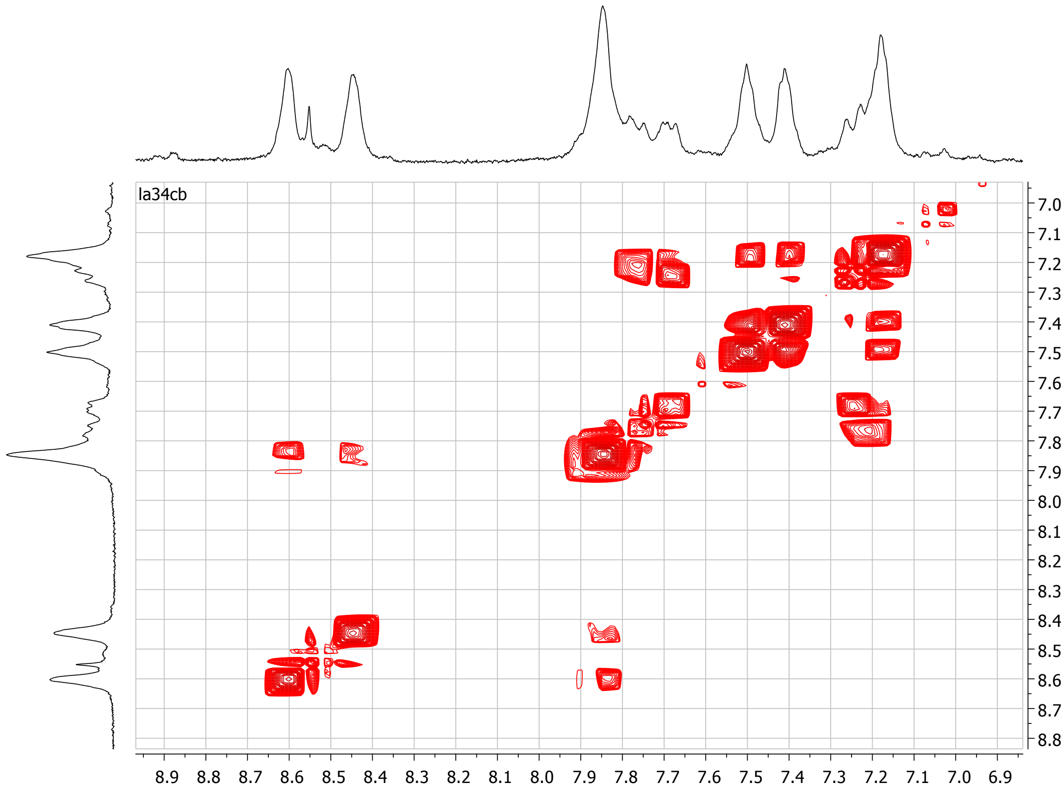

Figure S4. Fragments of the COSY spectrum of **1** in the presence of **CB[7]** (400 MHz, 298 K, D_2O-CD_3CN (3:1), $C_{\mathbf{1}}$ = $2\cdot10^{-3}$M, $C_{\mathbf{CB[7]}}$ = $1\cdot10^{-3}$M)

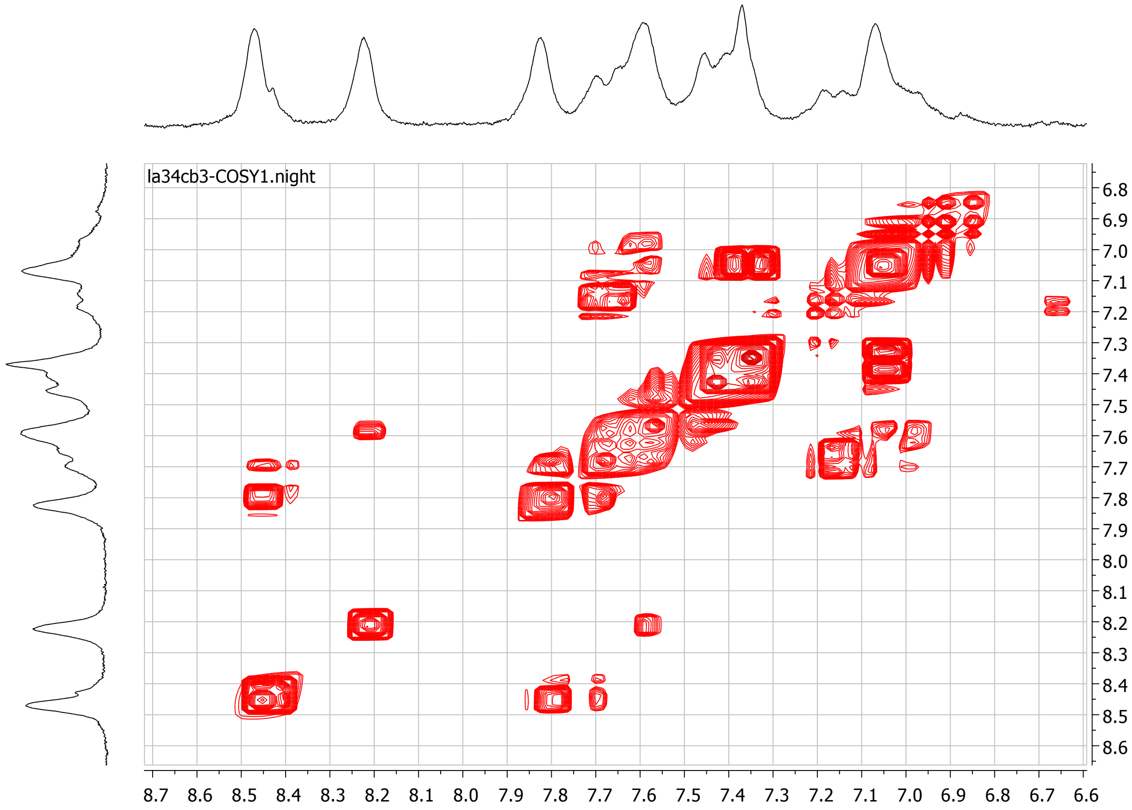

Figure S5. Fragments of the COSY spectrum of **1** in the presence of **CB[7]** (400 MHz, 298 K, D_2O-CD_3CN (3:1), $C_1 = 2\cdot10^{-3}$M, $C_{CB[7]} = 2\cdot10^{-3}$M)

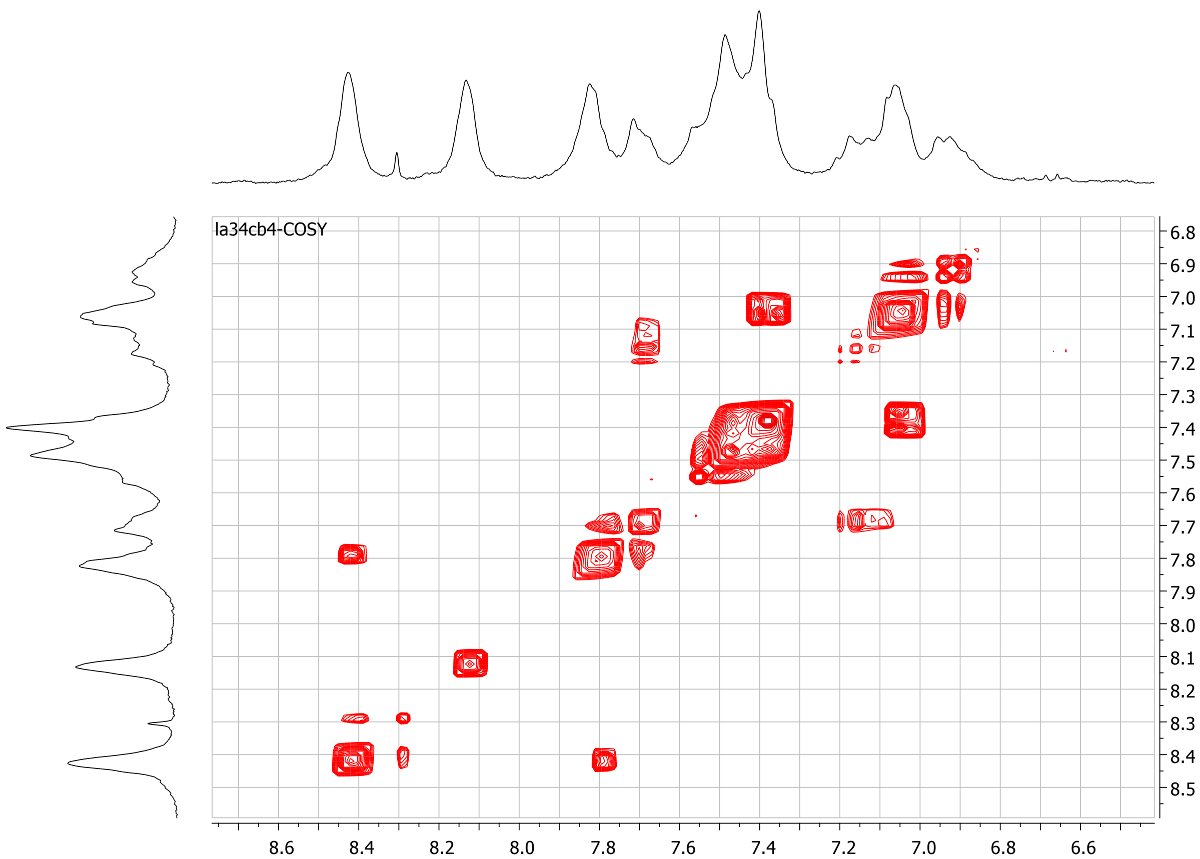

Figure S6. Fragments of the COSY spectrum of **1** in the presence of **CB[7]** (400 MHz, 298 K, D_2O-CD_3CN (3:1), $C_1 = 2\cdot10^{-3}$M, $C_{CB[7]} = 3\cdot10^{-3}$M)

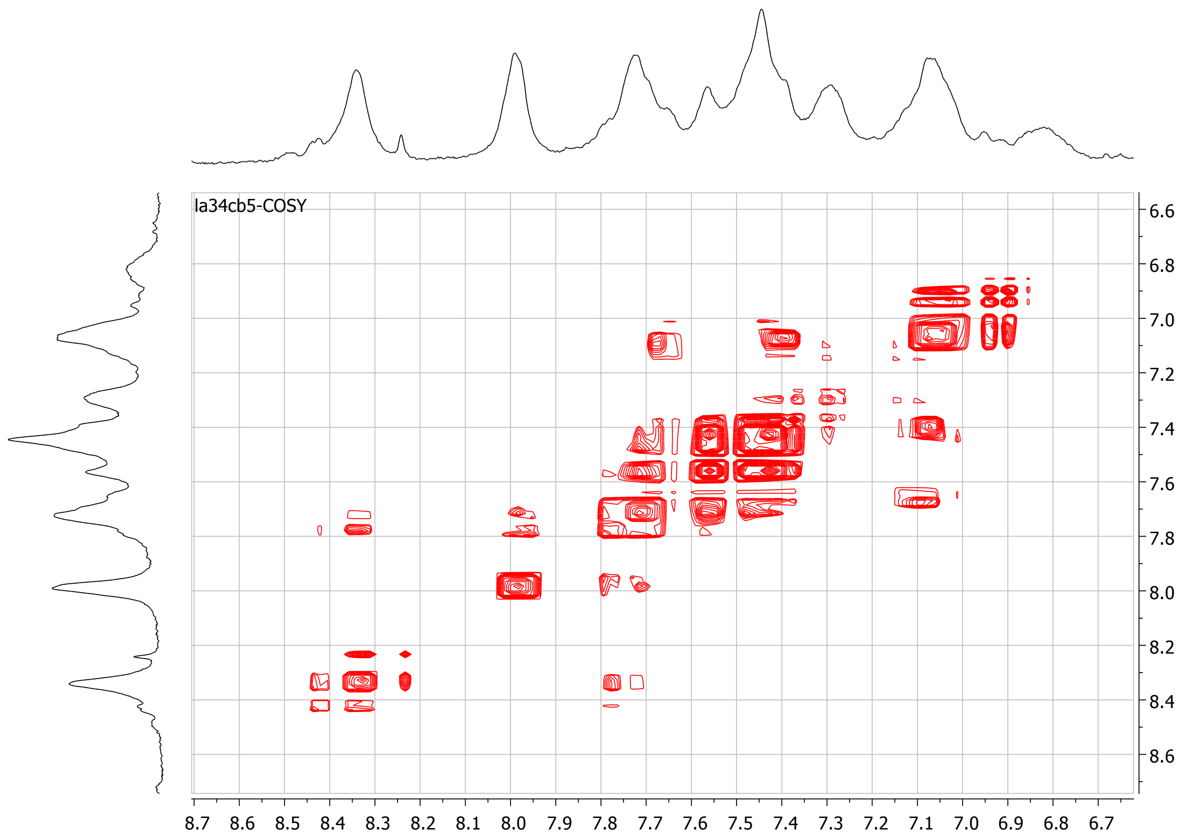

Figure S7. Fragments of the COSY spectrum of **1** in the presence of **CB[7]** (400 MHz, 298 K, D_2O-CD_3CN (3:1), $C_1 = 2\cdot10^{-3}$M, $C_{CB[7]} = 5\cdot10^{-3}$M)

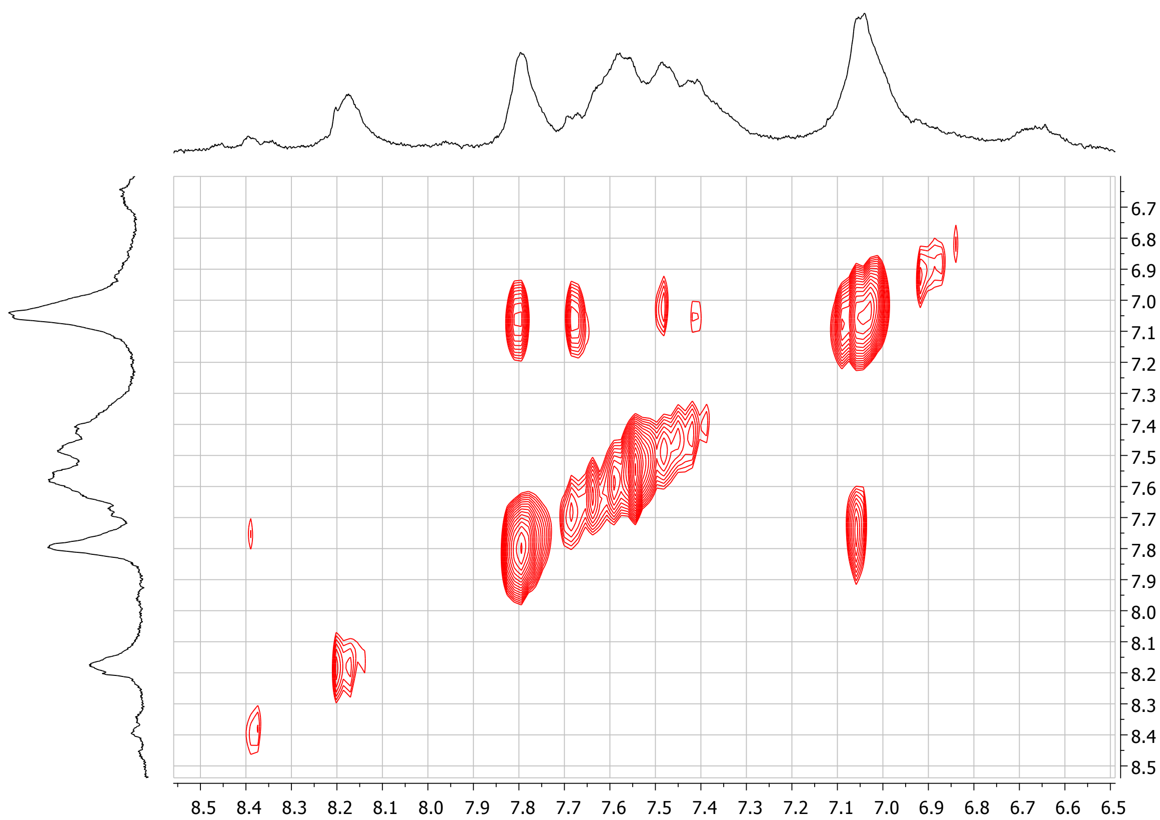

Figure S8. Fragments of the COSY spectrum of **1** in the presence of **CB[7]** (400 MHz, 298 K, D_2O-CD_3CN (3:1), $C_1 = 2\cdot10^{-3}$M, $C_{CB[7]} = 1\cdot10^{-2}$M)

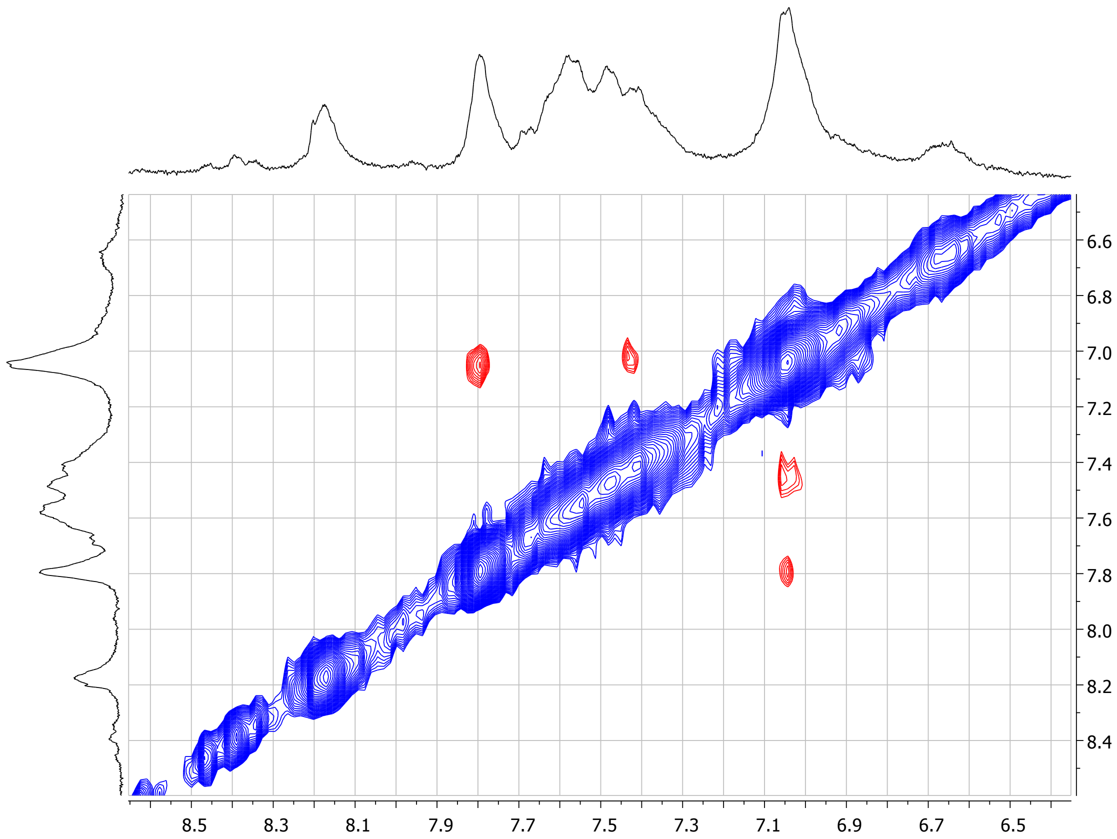

Figure S9. Fragments of the ROESY spectrum of **1** in the presence of **CB[7]** (400 MHz, 298 K, D_2O-CD_3CN (3:1), $C_1 = 2 \cdot 10^{-3}$M, $C_{CB[7]} = 1 \cdot 10^{-2}$M)

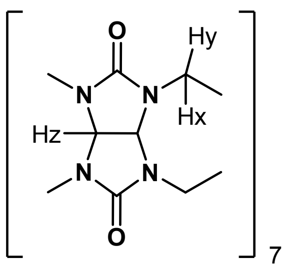

CB[7]

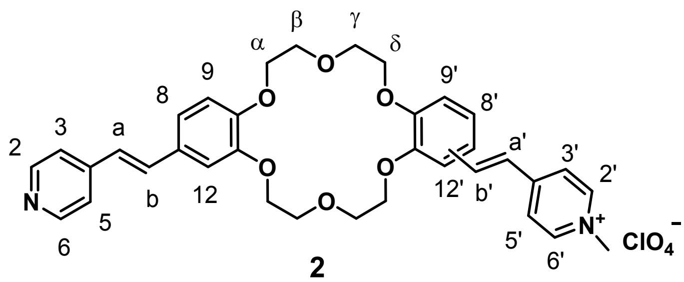

2

CB[7]. $C_{CB[7]} = 1 \cdot 10^{-3}$M. ^{1}H NMR (400 MHz, D_2O:CD_3CN (3:1), δ, ppm): 4.32 (d, 14H, H(y), J = 15.3), 5.59 (s, 14H, H(z)), 5.99 (d, 14H, H(x), J = 15.3).

Dye 1. $C_1 = 2 \cdot 10^{-3}$M. ^{1}H NMR (400 MHz, D_2O:CD_3CN (3:1), δ, ppm): 4.17-4.01 (m, 8H, H-β, H-γ); 4.35 (s, 3H, CH_3), 4.43-4.30 (m, 8H, H-α, H-δ), 7.24-7.13 (m, 3H, H-9, H-9', H-a), 7.49-7.29 (m, 5H, H-8, H-12, H-a', H-8', H-12'), 7.56 (d, 1H, H-b, J_{trans} = 16.4), 7.67 (d, 2H, H-3, H-5, J = 5.5), 7.86 (d, 1H, H-b', J_{trans}= 16.0), 8.08 (d, 2H, H-3', H-5', J = 6.6), 8.64-8.56 (m, 4H, H-2', H-6', H-2, H-6).

Mixture dye 1 and CB[7] (1:0.5). C_1 = 2·10^{-3}M, $C_{CB[7]}$ = 1·10^{-3}M. ^{1}H NMR (400 MHz, $D_2O:CD_3CN$ (3:1), δ, ppm): 4.18-4.06 (m, 8H, H-β, H-γ), 4.44-4.26 (m, 25H, H(y),CH_3,H-α, H-δ), 5.59 (s, 14H, H(z)), 5.99 (d, 14H, H(x), J= 15.3), 7.29-7.11 (m, 4H, H-9, H-9', H-a, H-a'), 7.45-7.35 (m, 2H, H-8, H-12), 7.56-7.46 (m, 2H, H-8', H-12'), 7.79 (d, 1H, H-b, J_{trans} = 15.9), 7.77 (d, 1H, H-b', J_{trans}= 15.5), 7.94-7.80 (m, 4H, H-3, H-5, H-3', H-5'), 8.45 (br. s, 2H, H-2', H-6'), 8.60 (br. s, 2H, H-2, H-6).

Mixture dye 1 and CB[7] (1:1). C_1 = 2·10^{-3}M, $C_{CB[7]}$ = 2·10^{-3}M. ^{1}H NMR (400 MHz, $D_2O:CD_3CN$ (3:1), δ, ppm): 4.19-4.06 (m, 8H, H-β, H-γ), 4.42-4.24 (m, 25H, H(y), CH_3,H-α, H-δ), 5.59 (s, 14H, H(z)), 5.89 (d, 14H, H(x), J= 15.2), 7.21-7.04 (m, 3H, H-a', H-9, H-9'), 7.27 (d, 1H, H-a, J_{trans} = 16.0), 7.60-7.39 (m, 4H, H-8, H-12, H-8', H-12'), 7.86-7.64 (m, 4H, H-3', H-5', H-b, H-b'), 7.93 (br. s, 2H, H-3, H-5), 8.33 (br. s, 2H, H-2', H-6'), 8.58 (br. s, 2H, H-2, H-6).

Mixture dye 1 and CB[7] (1:1.5). C_1 = 2·10^{-3}M, $C_{CB[7]}$ = 3·10^{-3}M. ^{1}H NMR (400 MHz, $D_2O:CD_3CN$ (3:1), δ, ppm): 4.19-4.06 (m, 8H, H-β, H-γ), 4.42-4.22 (m, 25H, H(y), CH_3,H-α, H-δ), 5.58 (s, 14H, H(z)), 5.87 (d, 14H, H(x), J= 15.6), 7.05 (d, 1H, H-a', J_{trans} = 16.4), 7.34-7.10 (m, 3H, H-9, H-9', H-a), 7.72-7.42 (m, 7H, H-8, H-12, H-8', H-12', H-3', H-5', H-b'), 7.81 (d, 1H, H-b, J_{trans} = 16.4), 7.93 (br. s, 2H, H-3, H-5), 8.24 (br. s, 2H, H-2', H-6'), 8.54 (br. s, 2H, H-2, H-6).

Mixture dye 1 and CB[7] (1:2.5). C_1 = 2·10^{-3}M, $C_{CB[7]}$ = 5·10^{-3}M. ^{1}H NMR (400 MHz, $D_2O:CD_3CN$ (3:1), δ, ppm): 4.19-4.06 (m, 8H, H-β, H-γ), 4.42-4.22 (m, 25H, H(y), CH_3,H-α, H-δ), 5.58 (s, 14H, H(z)), 5.87 (d, 14H, H(x), J= 15.6), 6.93 (br. s, 1H, H-a'), 7.29-7.08 (m, 3H, H-9, H-9', H-a), 7.40 (br. s, 2H, H-3', H-5'), 7.92-7.46 (m, 8H, H-8, H-12, H-8', H-12', H- b, H-b', H-3, H-5), 8.10 (br. s, 2H, H-2', H-6'), 8.54 (br. s, 2H, H-2, H-6).

Mixture dye 1 and CB[7] (1:5). C_1 = 2·10^{-3}M, $C_{CB[7]}$ = 1·10^{-2}M. ^{1}H NMR (400 MHz, $D_2O:CD_3CN$ (3:1), δ, ppm): 4.20-4.05 (m, 8H, H-β, H-γ), 4.42-4.22 (m, 25H, H(y), CH_3,H-α, H-δ), 5.56 (s, 14H, H(z)), 5.85 (d, 14H, H(x), J= 15.2), 6.78 (br. s, 1H, H-a'), 7.28-7.03 (m, 6H, H-9, H-9', H-a, H-3', H-5', H-b'), 7.83-7.40 (m, 7H, H-8, H-12, H-8', H-12', H- b, H-3, H-5), 7.92 (br. s, 2H, H-2', H-6'), 8.30 (br. s, 2H, H-2, H-6).

Electrochemistry studies

Electrochemical measurements were carried out at 22 ˚C with an IPC-ProM potentiostat. Cyclic voltammetry experiments were performed in a 1.0 mL cell equipped with a glassy carbon (GC) electrode (disk d = 2 mm), Ag/AgCl/KCl (aq. saturated; reference electrode), and platinum electrode (counter electrode). Compounds were dissolved in degassed dry CH_3CN or DMF containing TBAP as the supporting electrolyte (0.1 M). Dry argon gas was bubbled through the solutions for 30 min before cyclic voltammetry experiments. The scan rate was 200 mV s^{-1}.

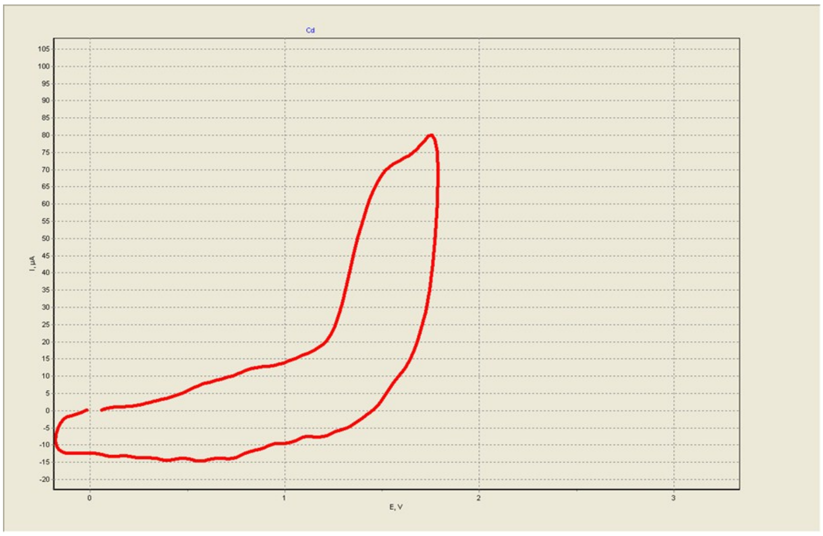

Fig. S10. Cyclic voltammograms of **3** obtained on GC electrode, E_0=1.48V 57mkA.

Fig. S11. Cyclic voltammograms of **3** obtained on GC electrode, E_0= -1.03V 12mkA.

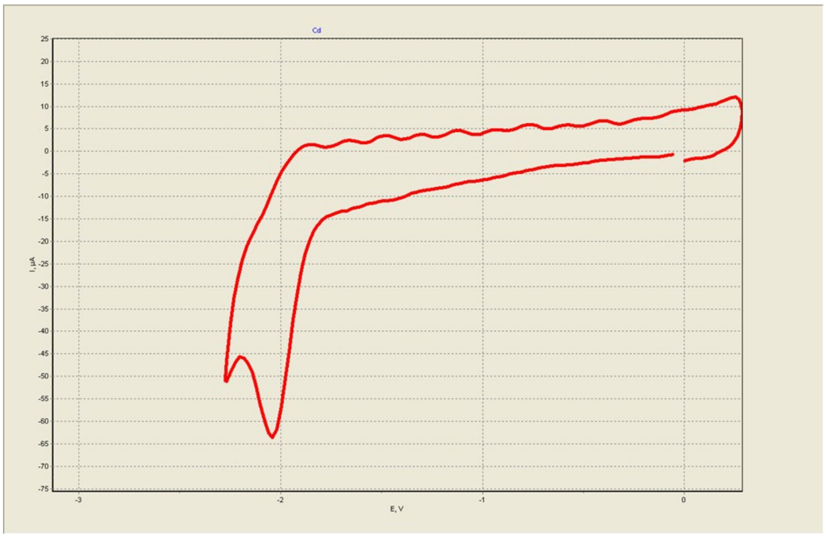

Fig. S12. Cyclic voltammograms of **2** obtained on GC electrode, E_0=-1.98V 51mkA

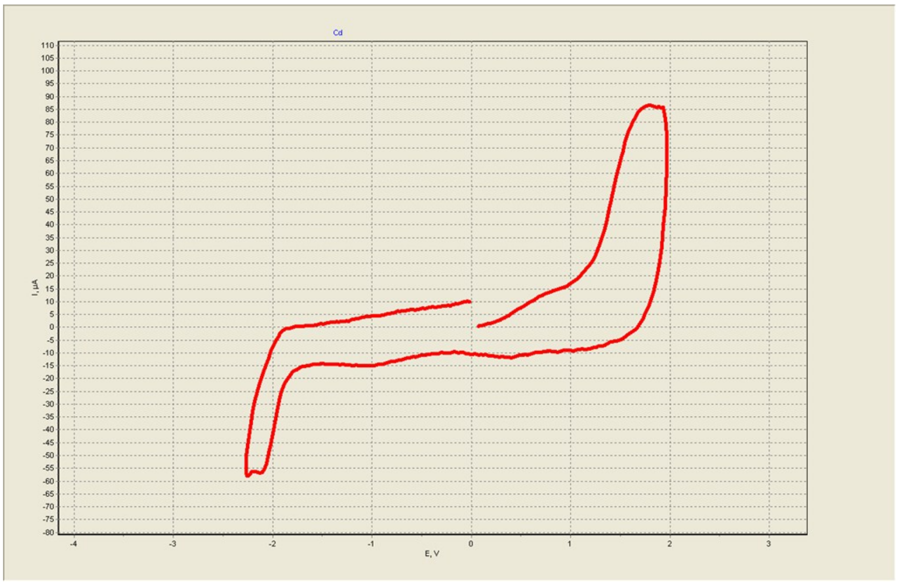

Fig. S13. Cyclic voltammograms of **2** obtained on GC electrode, E_0=-1.98V 42mkA

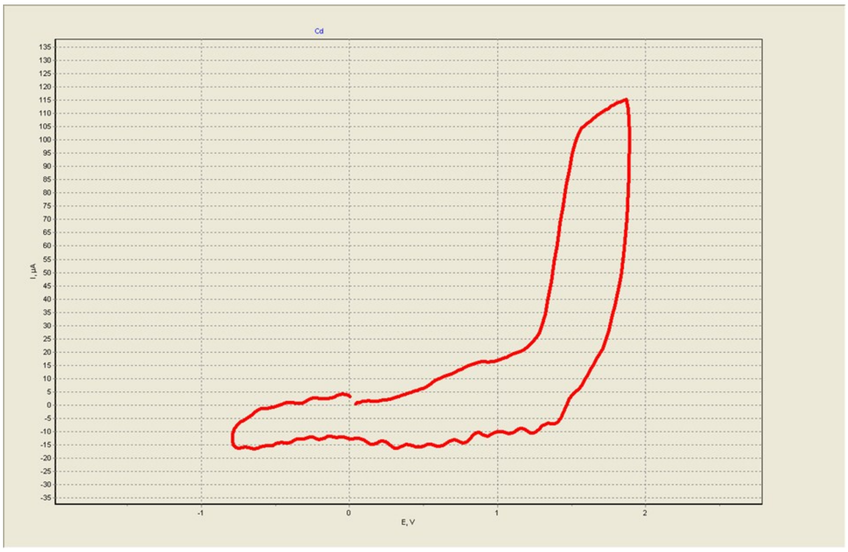

Fig. S14. Cyclic voltammograms of **1** obtained on GC electrode, E_0= 1.57V 87mkA

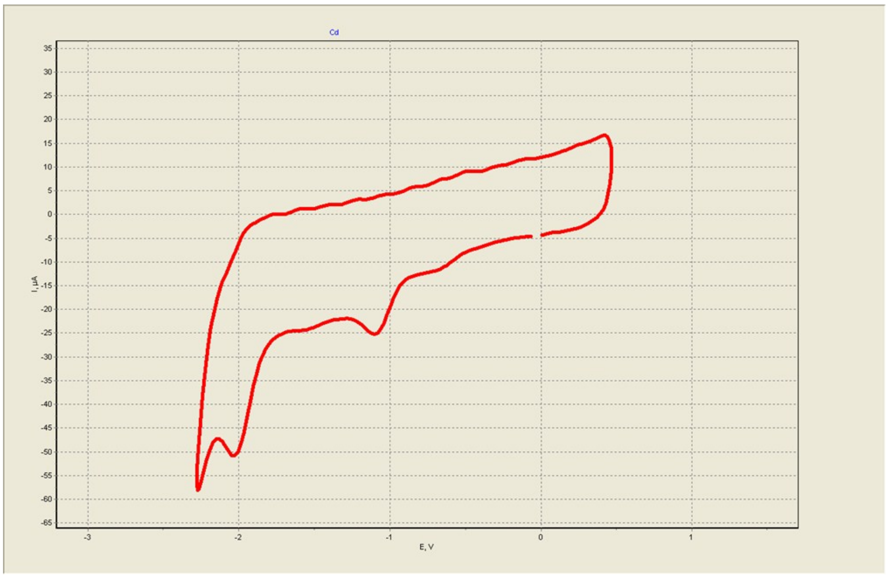

Fig. S15. Cyclic voltammograms of **1** obtained on GC electrode, E_0= -1.02V 13mkA 2.E_0=-1.97V 29mkA.

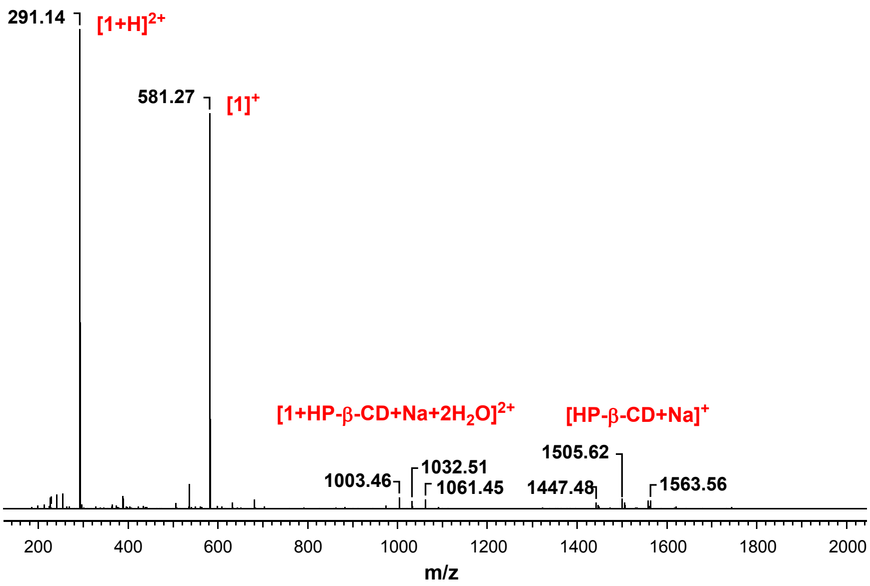

Fig. S16. – Mass-spectrum of **1** (C_1 = 2·10^{-5}M) in the presence of **HP-β-CD** ($C_{HP\text{-}\beta\text{-}CD}$ = 1·10^{-4}M) and NaClO$_4$(C_{NaClO4} = 4·10^{-5}M) in water.

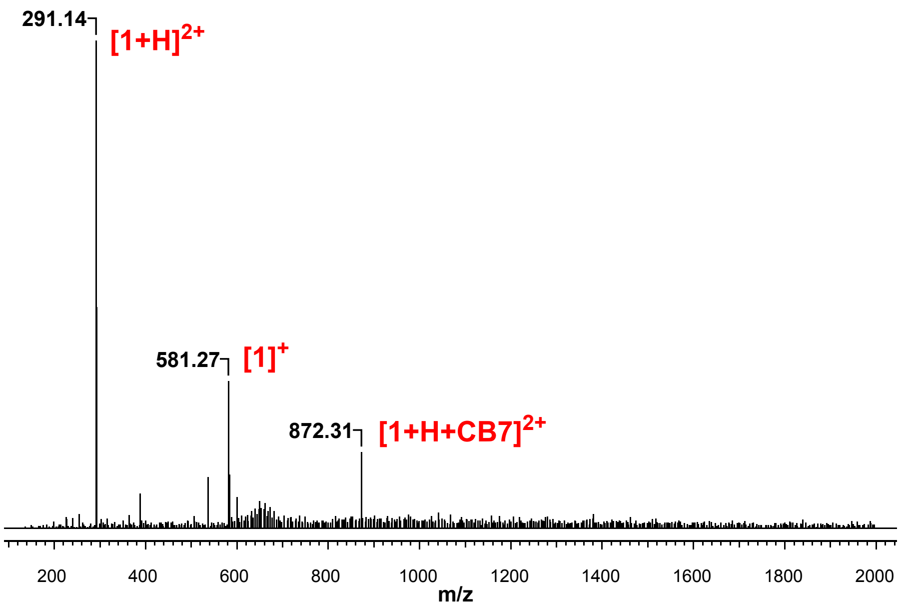

Fig. S17. – Mass-spectrum of **1** (C_1 = 2·10^{-5}M) in the presence of **CB[7]** ($C_{CB[7]}$ = 1·10^{-5}M) and NaClO$_4$ (C_{NaClO4} = 4·10^{-5}M) in water.

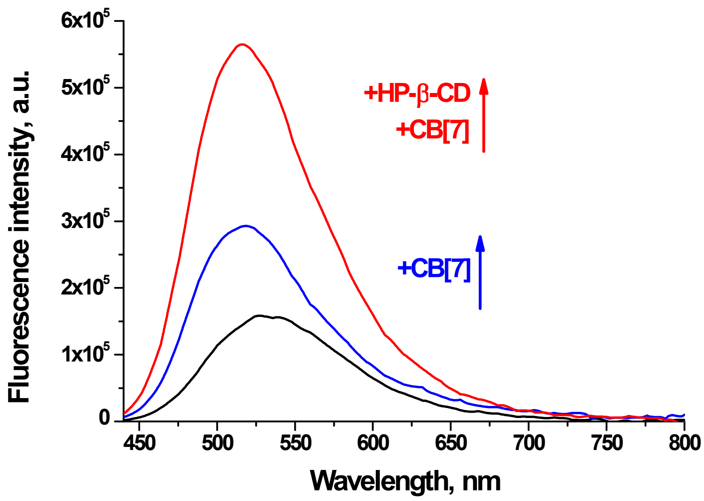

Fig. S18. – Fluorescence emission spectra of free **1** (black) and in the presence of: 7·10^{-4} M **CB[7]** (blue), 1.5·10^{-2} M **HP-β-CD** and 7·10^{-4} M **CB[7]** (red) in borax buffer (pH = 9.4). Temperature 298 K, excitation at 430 nm, in all cases C_1 = 1.0·10^{-5}M.

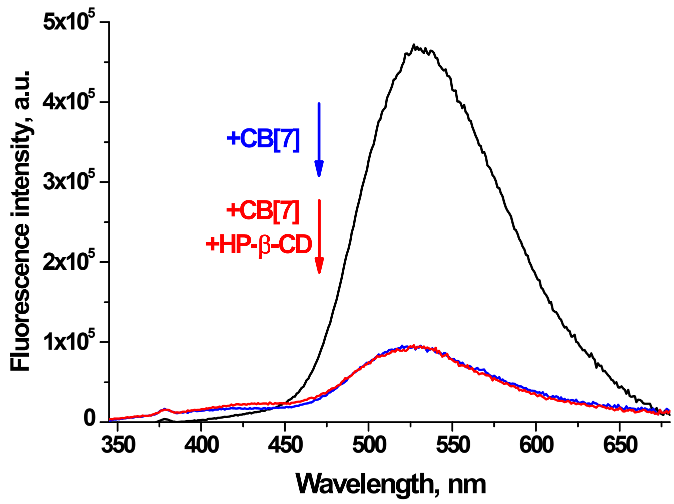

Fig. S19. – Fluorescence emission spectra of free **1** (black) and in the presence of: 5·10^{-4} M **CB[7]** (blue), 1.5·10^{-2} M **HP-β-CD** and 5·10^{-4} M **CB[7]** (red) in borax buffer (pH = 9.4). Temperature 298 K, excitation at 335 nm, in all cases C_1 = 1.0·10^{-5}M.

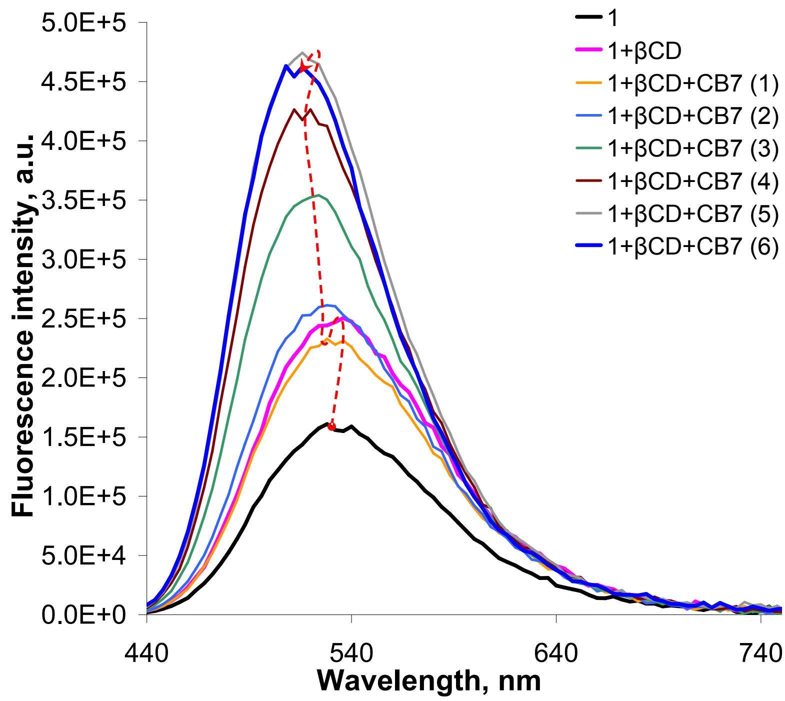

Fig. S20. Fluorescence emission spectra of free **1** (black) (C_1=9.8·10^{-6} M) and in the presence of: **HP-β-CD** (pink) (C_1=9.8·10^{-6} M, $C_{βCD}$=2.2·10^{-3} M), **HP-β-CD** and **CB[7]** (blue) (C_1=7.9·10^{-6} M, $C_{βCD}$=1.7·10^{-3} M, C_{CB7}=3.9·10^{-4} M) in borax buffer (pH = 9.4). Temperature 298 K, excitation at 430 nm.

a)

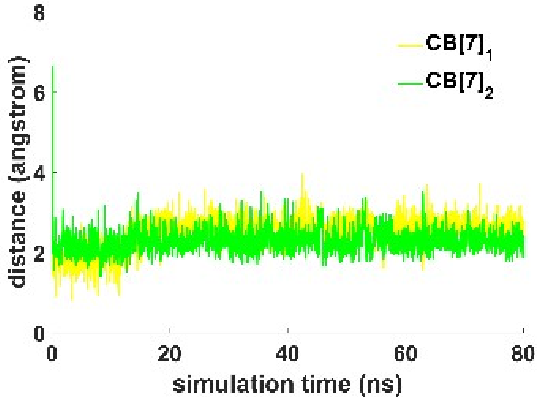

CB[7]$_1$
CB[7]$_2$
distance (angstrom)
simulation time (ns)
0
2
4
6
8
0
20
40
60
80

b)

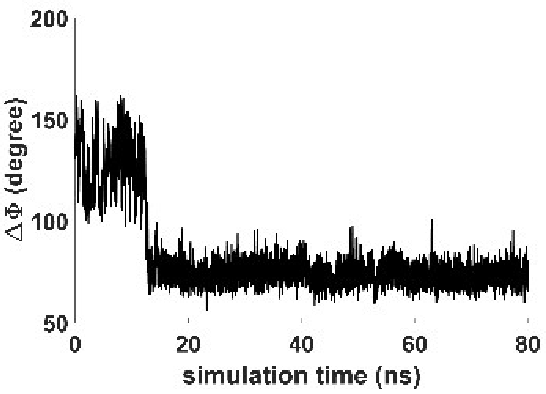

ΔΦ (degree)
simulation time (ns)
50
100
150
200
0
20
40
60
80

c)

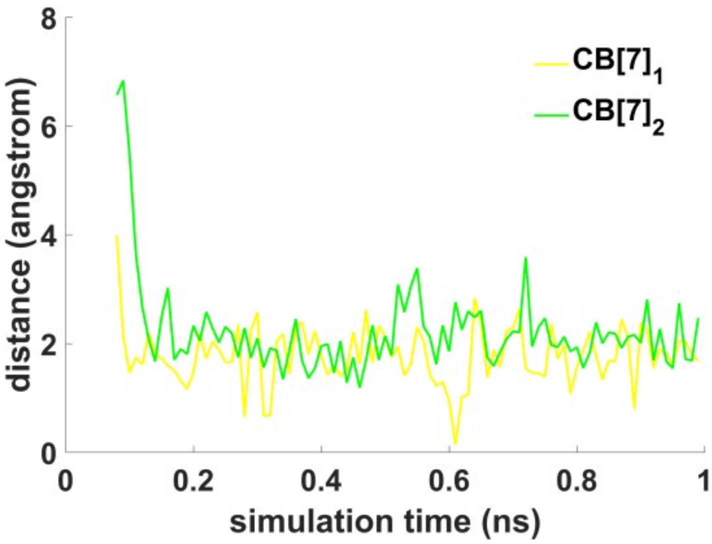

CB[7]$_1$
CB[7]$_2$
distance (angstrom)
simulation time (ns)
0
2
4
6
8
0
0.2
0.4
0.6
0.8
1

d)

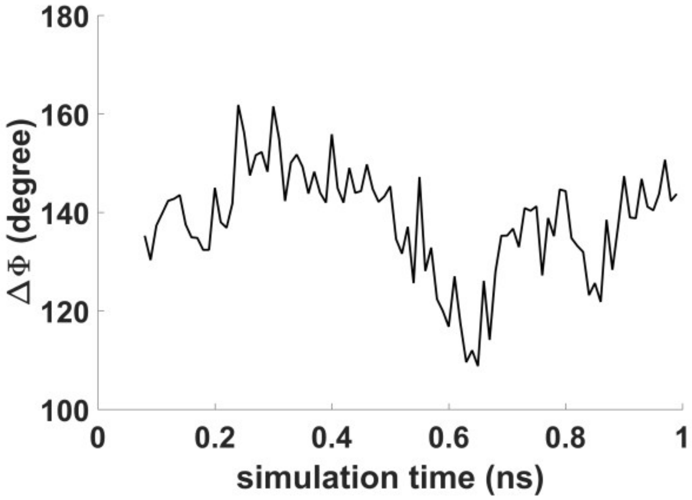

Fig.S21 a) The evolution of the distance between mass centers of terminal pyridine moieties and carbonyl portals of CB[7], farthest from the N-atoms; b) The evolution of the angle between the vector connecting the centers of mass of the terminal pyridine moieties and the center of mass of oxygen atoms of 18-crown-6 ether; c) and d) The evolution of the data presented in Fig. S21a,b at the initial stage of calculations with a duration of 1 ns.

a)

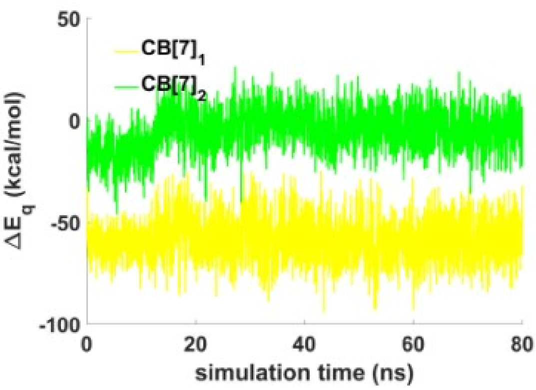

b)

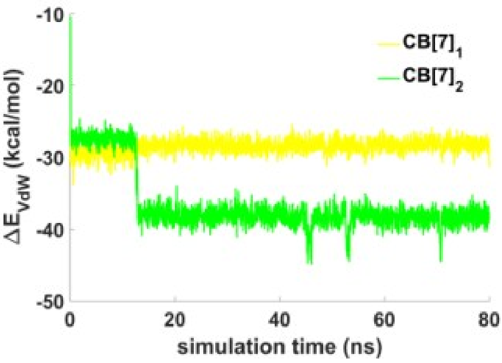

c)

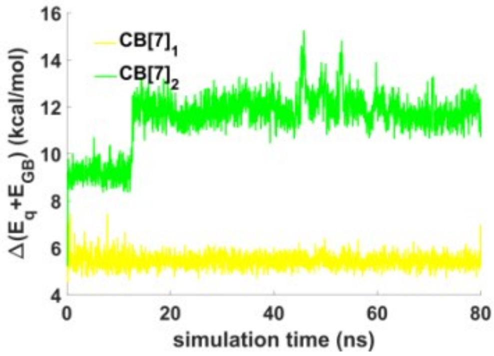

d)

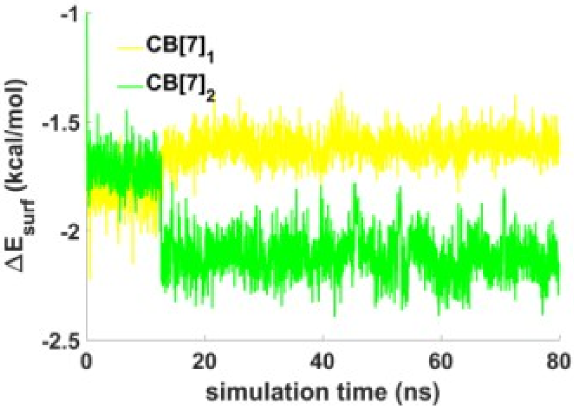

Fig.S22 a) This is the contribution of E_q; b) is the sum of E_q and E_{GB}; c) is the contribution of E_{vdw}; d) is the contribution of E_{surf}. The line marked as $CB[7]_1$ refers to the interaction of CB[7] with N-methyl-4-styryl-pyridinium residue; the line marked as $CB[7]_2$ refers to the interaction of CB[7] with 4-styryl-pyridine residue, all in the complex $1@(CB[7])_2$.

a) b)

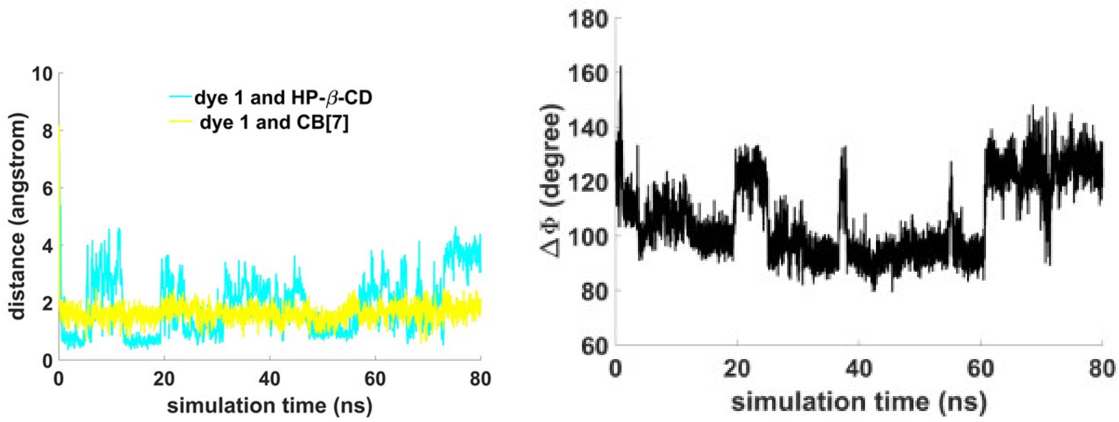

Fig. S23 a) The evolution of the distance between mass centers of terminal pyridine moieties and carbonyl portals in case of CB [7], and the center of mass of the oxygen in the hydroxyl groups of the pyranoses in case of HP-β-CD., farthest from the N-atoms; b) The evolution of the angle between the vector connecting the centers of mass of the terminal pyridine moieties and the center of mass of oxygen atoms of 18-crown-6 ether.

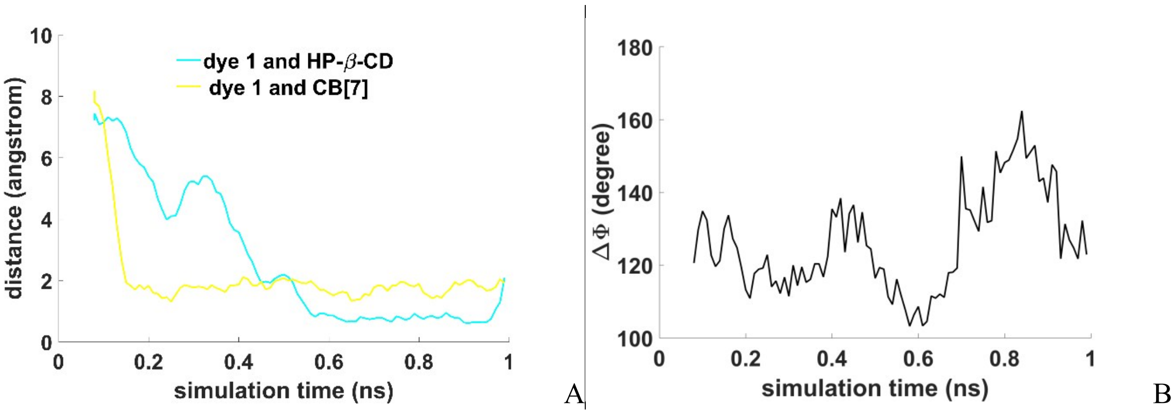

Fig.S24 The evolution of the data presented in Fig. 13 at the initial stage of calculations at duration of 1 ns.

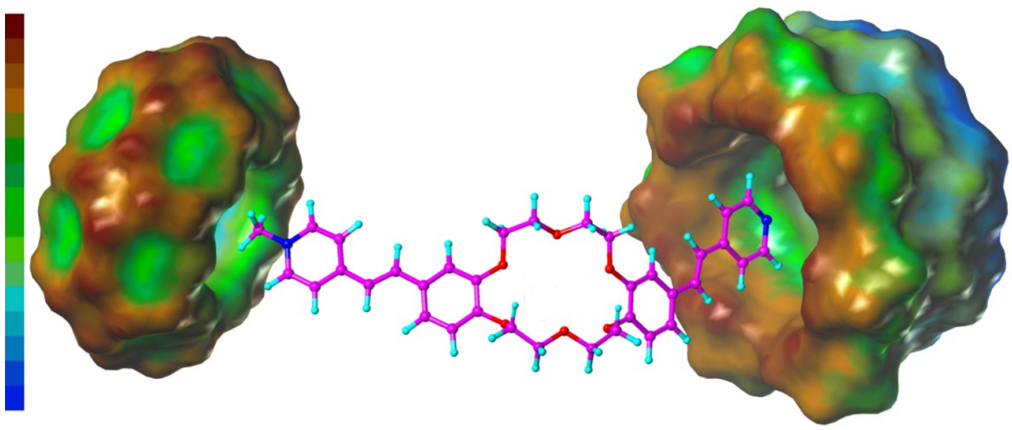

Fig.S25 Starting position of components of dye 1, CB[7] and HP-β-CD molecules relative to each other. The CB[7] and HP-β-CD are covered with a Connolly surface, which is colored depending on the distribution of the hydrophobic potential from smallest (blue) to (brown).

a)

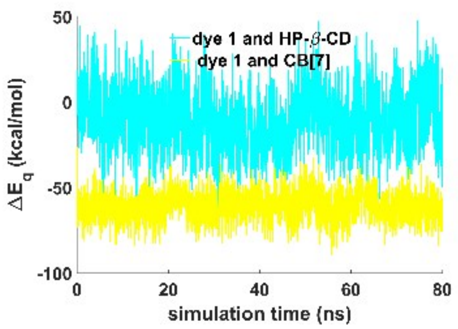

b)

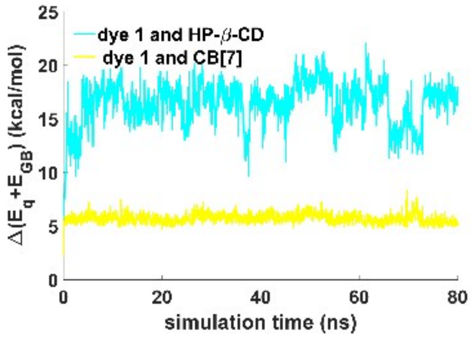

c)

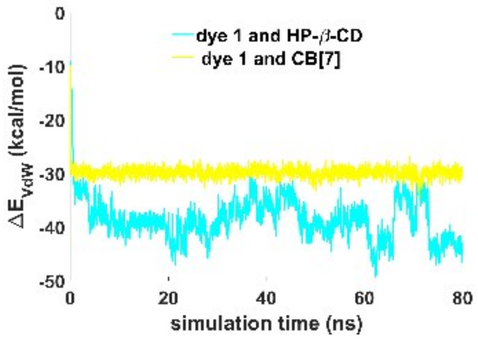

d)

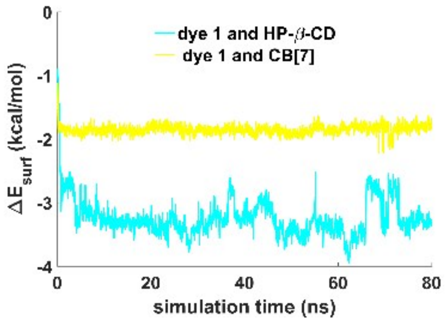

Fig. S26 a) This is the contribution of E_q; b) is the sum of E_q and E_{GB}; c) is the contribution of E_{vdw}; d) is the contribution of E_{surf}. The line marked as (dye **1** and HP-β-CD) refers to the interaction of HP-β-CD with 4-styryl-pyridine residue; and the line marked as (dye **1** and CB[7]) refers to the interaction of CB[7] with N-methyl-4-styryl-pyridinium residue, all in the complex HP-β-CD@1@CB[7].

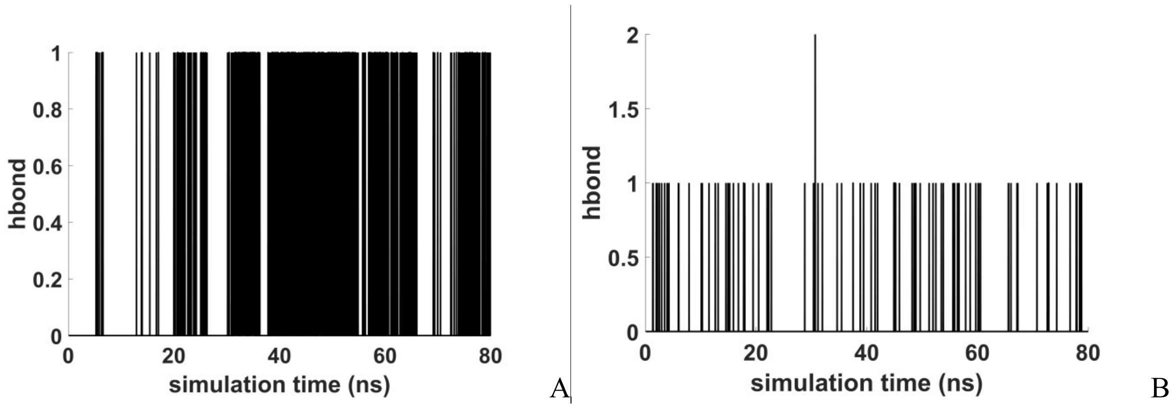

Fig. S27 (A) – The evolution of the amount of hydrogen bonds between CB[7] and HP-β-CD. (B) - The evolution of the amount of hydrogen bonds between dye 1 and HP-β-CD.